LA-UR-81-1694

TITLE: IMPROVED CALCULATIONS OF ENERGY DEPOSITION FROM FAST NEUTRONS

AUTHOR(S): D. J. Brenner, R. E. Prael, J. F. Dicello, and M. Zaider

SUBMITTED TO: 4th Symposium on Neutron Dosimetry, Neuherberg/Munich
June 1981

University of California

LOS ALAMOS SCIENTIFIC LABORATORY
Post Office Box 1663 Los Alamos, New Mexico 87545
An Affirmative Action/Equal Opportunity Employer

IMPROVED CALCULATIONS OF ENERGY DEPOSITION FROM FAST NEUTRONS

D. J. Brenner, R. E. Prael, J. F. Dicello, and M. Zaider*
Los Alamos National Laboratory
Los Alamos, NM 87545 USA

ABSTRACT

Increased interest in fast neutrons for radiotherapy has led to a need for accurate measurements and calculations in the energy region up to 100 MeV. Experimental neutron cross sections on elements of biological interest in the region above 15 MeV are sparse. Moreover, until recently, no secondary particle production spectra had been measured in this energy range. New data from the University of California at Davis has allowed cross-sectional calculations to be more firmly based. This in turn results in improved calculations of dose and energy deposition in small sites from high-energy neutrons.

Secondary particle production spectra due to neutrons incident on carbon and oxygen are calculated using an intranuclear cascade code which takes into account specific nuclear properties of carbon and oxygen (in particular, alpha-particle clustering). It also allows excited nuclei to deexcite by Fermi breakup rather than the more frequently used statistical evaporation mechanism, which is not applicable to low-mass nuclei. The code yields double-differential secondary particle spectra in energy and angle which show good agreement with the experimental data from the University of California at Davis at 27, 40, and 61 MeV.

The use of these complete theoretical cross-section data allow, for example, the calculation of absolute depth-dose curves for particular beams, as opposed to depth-kerma curves which are less sensitive to secondary particle distributions. These calculations are performed with a Monte Carlo neutron transport code; buildup curves which are sensitive to secondary charged particle distributions are calculated for high energy neutron beams (e.g., p(65)-Be).

The cross-sectional data set also allows the calculation of energy-deposition distributions in small sites, these distributions being even more sensitive to the secondary particle spectra. Microdosimetric lineal energy spectra are calculated with Monte Carlo techniques reported previously using as input measured neutron energy spectra. As an example, the lineal energy spectra from p(65)-Be and 20 MeV monoenergetic neutrons in a 2-μm site size show excellent agreement with experiment.

Current address: Radiological Research Laboratory, Columbia University, New York, NY

Introduction

The increase in interest in fast neutron radiotherapy in USA and Europe has focused attention on the lack of reliable neutron cross-sectional data above 15 MeV. Possible theoretical techniques for predicting these cross-sections for carbon, oxygen, and nitrogen have been reviewed by Jackson and Brenner.[1] In light of this work, it is clear that calculation specific to light nuclei must be used. We have, therefore, chosen to refine an intranuclear cascade and deexcitation model putting in specific nuclear data to make the deexcitation as realistic as possible.

Theory of the Cascade and Breakup Models

The calculations described in this paper have been performed with two codes designated INCA1 and INCA2. Originally obtained from the University of Maryland,[2] the two codes have been extensively rewritten, modified and extended at Los Alamos. INCA1 is an intranuclear cascade code based on the well-known VEGA3[3] code. INCA2 is a code to calculate the deexcitation of light nuclei by the Fermi breakup model.

INCA1 is based on the scheme presented by Chen[4] with the following different features:

1) it lacks the pion physics of the VEGAS code, and thus is useful only below the pion production threshold.
2) a treatment of alpha and deuteron clusters, with user specified spectroscopic parameters;
3) among other options, the nuclear density may be described by a three-parameter Fermi distribution or a harmonic well.

At the present time, the cluster treatment is rather limited and unrealistic in that the clusters are treated as fermions. The breakup of the clusters within the nucleus is allowed, but the method has not been closely examined. An improved quantum-mechanical treatment of clusters is planned.

INCA2 is used to calculate the deexcitation of the residual nuclei obtained from INCA1. The formulation follows the prescription of Epherre[4], with channel probabilities and particle momenta determined by phase space considerations. However, a number of features have been included to supplement the basic Fermi breakup model:

1. up to seven-body breakup modes are allowed;
2. particle-unstable levels are allowed as intermediate states, thus permitting sequential decay processes;
3. two-body breakup channels use a Coulomb barrier penetration factor approximated from Coulomb wave functions, while multiparticle modes use a breakup threshold adjusted for Coulomb energy;
4. two-body breakup of levels with known spin and parity are restricted to conserve parity and are inhibited by neutral particle angular momentum barrier penetration factors.

Although the two codes have several adjustable parameters, perhaps the most sensitive are the cutoff parameters to specify the minimum energy a particle may have to escape during the cascade. High cutoffs favor compound nucleus formation, while low cutoffs favor direct reactions in the

cascade stage. In the calculations described below, the cutoff energies for the charged particles was taken to be 1 MeV above the Coulomb barrier, while 3 MeV was used as a neutron cutoff. The calculation employed a time average of one alpha cluster plus eight nucleons in ^{12}C.

Results of the Cascade

In Fig. 1, the calculated nonelastic and (n,n′)3α sections for neutrons on ^{12}C are shown. The nonelastic cross section agrees fairly well with experimental results above 40 MeV, but is noticeably smaller than the ENDF-B/V evaluation below 20 MeV, as is the (n,n′)3α cross section. The overestimation of α particle production at 20 MeV by the ENDF-B/V evaluation has been qualitatively inferred by McDonald et al.[5] In Fig. 2, angle-integrated secondary particle production cross sections at 40 MeV are shown and compared with the experimental data of Brady and Romero.[6] These figures illustrate some general trends in the calculation over the whole energy range of interest:

1. generally good agreement is obtained for protons, tritons, and alpha particles at 27, 40, and 61 MeV;
2. calculated results for alpha particles are somewhat low at high energies;
3. the lack of a model for pickup reactions leads to deuteron production rates that are a factor of 3 to 5 too low over this energy region.

We have also calculated double-differential particle production spectra which show the same trends and about the same degree of agreement as the angle-integrated data. As an example we show in Fig. 3 the proton spectra at two angles resulting from 61 MeV neutrons incident on ^{12}C.

In Fig. 4, the calculated kerma factors for ^{12}C are shown over the energy region 10 MeV to 100 MeV. The results include the contribution from all heavy fragments and an elastic recoil contribution calculated by Herling and Bassel.[7] In Table 1, the calculated contributions of various particles to the kerma factor are compared to experiment. In addition, the results of calculations forcing the breakup to go entirely by the compound nucleus ^{13}C (an approach used, for example, by Dimbylow[8]) are shown; the individual contributions show much less agreement with experiment.

Energy Deposition Calculation Technique

The production of reliable cross sections for secondary-particle production allows us to perform improved calculations of depth-dose curves, buildup curves, and microdosimetric spectra. Our techniques have been described earlier[9]: in essence, a pointwise Monte Carlo approach is used in which an experimentally determined energy spectrum of neutrons is transported and the resultant heavy charged particles are tracked from one ionizing collision to the next, the secondary and higher generation delta-ray tracks which cause straggling also being followed using Monte Carlo methods. The differential production cross sections for delta rays were estimated by assuming that delta-ray formation processes for given ion values of z and β (i.e., charge and speed) are the same as for electrons except for a scaling factor of z^2. The primary electron data were obtained as in Ref. 9. We intend to incorporate recent data on delta-ray production in ion atom collision (e.g., Ref. 10) into our calculation which will

remove some of the uncertainties associated with the scaling described above.

Results of Energy Deposition Calculations

In order to test our calculations at energies well above 20 MeV, we show some results for the p(66/65)-Be neutron beams at Fermilab/UC Davis. In both cases, the initial neutron energy spectrum was taken from measurements at UC Davis,[11] together with low energy neutron production data (< 10 MeV) taken from activation measurements in a d(40)-Be beam,[12] the latter measurement being normalized at 10 MeV to the former.

Figure 5 shows our calculations of the central-axis depth-dose curve in comparison with experiment. Figure 5a is absolutely normalized to the incident proton current, a feature not accomplished in other such calculations. The buildup region, shown in Fig. 5b shows moderate agreement with experiment.[13] Possible sources of part of the disagreement are external protons and photons originating in the target or collimator. Calculationally, the use of the d(40)-Be low-energy neutron spectrum below 10 MeV may be the source of some of the discrepancy. More recent experimental data from Fermilab[14] between 0.29 and 0.58 gm/cm^2 are, however, in significantly better agreement with the calculation. Figure 6 shows off-axis dose profiles under a 6 x 6 cm^2 collimator, which show good agreement with experiment.[15] The degree of agreement at distances from the axis greater than 6 cm (i.e., underneath the collimator) is surprising, indicating only a small contribution to the dose from the collimator itself. Figure 7 shows a comparison of calculated and experimental microdosimetric spectra for p(65)-Be and for 20 MeV monoenergetic neutrons. In both cases good agreement with experiment was obtained, in the latter case significantly better than the calculation of Caswell and Coyne[16] who used ENDF/B cross sections and did not take straggling into account.

Acknowledgements

The authors wish to thank Drs. Subramanian and Romero for providing us with their experimental data prior to publication, and Drs. Viola and Gokmen for providing us with their computer codes.

References

1. D. F. Jackson and D. J. Brenner, Prog. Part. Nucl. Phys. 5, 143 (1981).
2. B. G. Glagola et al., University of Maryland Cyclotron Laboratory Report, 1977.
3. K. Chen et al., Phys. Rev. 166, 949 (1968).
4. M. Epherre and E. Gradystajn, Journal de Physique 28, 747 (1967).
5. J. McDonald et al., Proc. 7th Symposium on Microdosimetry, Oxford, 1211 (1981).
6. F. Brady and J. Romero, Final Report to the National Cancer Institute, University of California, Davis (1979).
7. G. H. Herling and R. H. Bassel, private communication (May 1981).
8. P. J. Dimbylow, Phys. Med. Biol. 25, 637 (1980).
9. D. J. Brenner et al., Proc. 7th Symposium on Microdosimetry, Oxford, 677 (1981).

10. W. E. Wilson and L. H. Toburen, Proc. 7th Symposium on Microdosimetry, Oxford, 435 (1981).
11. H. I. Amols et al., Med. Phys. 4, 486 (1977).
12. L. R. Greenwood et al. Nucl. Sci. Eng. 72, 175 (1979).
13. M. Awschalom and I. Rosenberg, Med. Phys. 8, 105 (1981).
14. M. Awschalom, private communication (April 1981).
15. I. Rosenberg and M. Awschalom, Med. Phys. 8, 99 (1981).
16. R. S. Caswell and J. J. Coyne, see Ref. 5.

TABLE 1

Partial Kerma Factors for ^{12}C at 27.4 MeV(rad/(10^{19}/cm^2))

Particle	Experiment	Calc	Calc($^{13}C^*$)
p	0.37 ± 5%	0.326 ± 1. %	0.235 ± 1.2%
d	0.42 ± 20%	0.090 ± 1.1%	0.241 ± 1.1%
t	0.02 ± 20%	0.029 ± 1.6%	0.077 ± 1.6%
^{3}He	----	0.0034 ± 4%	0.0088 ± 4%
α	1.78 ± 5%	1.895 ± 0.5%	2.493 ± 0.5%
Nonelastic recoil	----	0.230 ± 0.6%	0.420 ± 0.9%
	Kerma for ^{12}C at 39.7		
p	0.89 ± 5%	0.792 ± 1.0%	0.330 ± 1.2%
d	0.62 ± 5%	0.121 ± 1.0%	0.431 ± 1.1%
t	0.10 ± 5%	0.106 ± 1.1%	0.420 ± 1.1%
^{3}He	0.08 ± 20%	0.034 ± 1.4%	0.093 ± 1.8%
α	1.45 ± 5%	1.403 ± 0.6%	1.961 ± 0.9%
Nonelastic recoil	----	0.380 ± 0.6%	0.792 ± 0.9%
	Kerma for ^{12}C at 60.7		
p	2.11 ± 5%	1.757 ± 0.9%	0.777 ± 1.1%
d	1.22 ± 5%	0.224 ± 1.1%	0.831 ± 1.2%
t	0.26 ± 20%	0.160 ± 1.2%	0.733 ± 1.1%
^{3}He	0.13 ± 20%	0.083 ± 1.5%	0.258 ± 1.5%
α	1.21 ± 5%	1.291 ± 0.7%	2.555 ± 1.0%
Nonelastic recoil	----	0.365 ± 0.7%	0.752 ± 1.1%

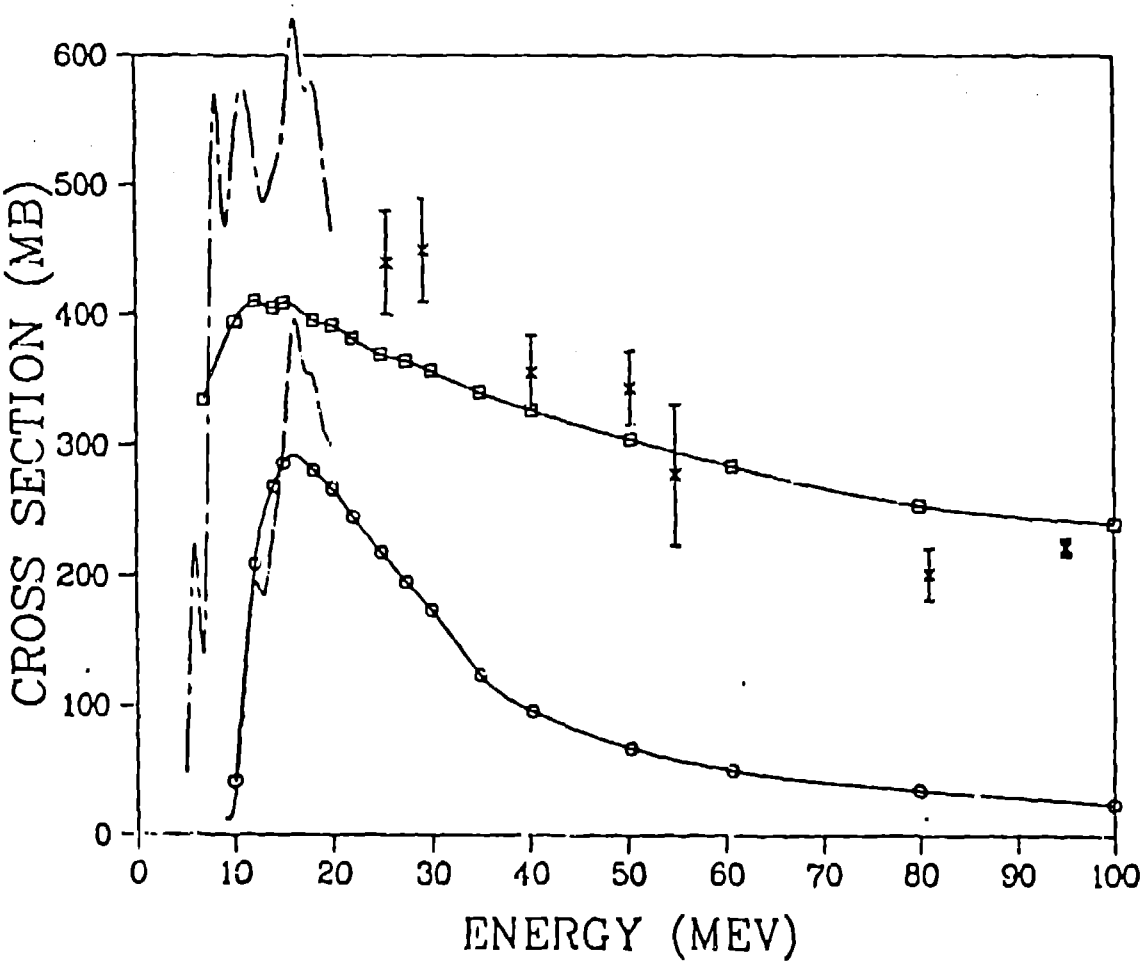

Fig. 1 Some partial cross-sections in ^{12}C:
Upper Full Line: Calculated nonelastic cross section.
Upper Dashed Curve: ENDF-B/V evaluation of nonelastic cross section.
Lower Full Line: Calculated (n,n')3α cross section.
Lower Dot-Dash Curve: ENDF-B/V evaluation of (n,n')3α cross section. The crosses are experimental data points.

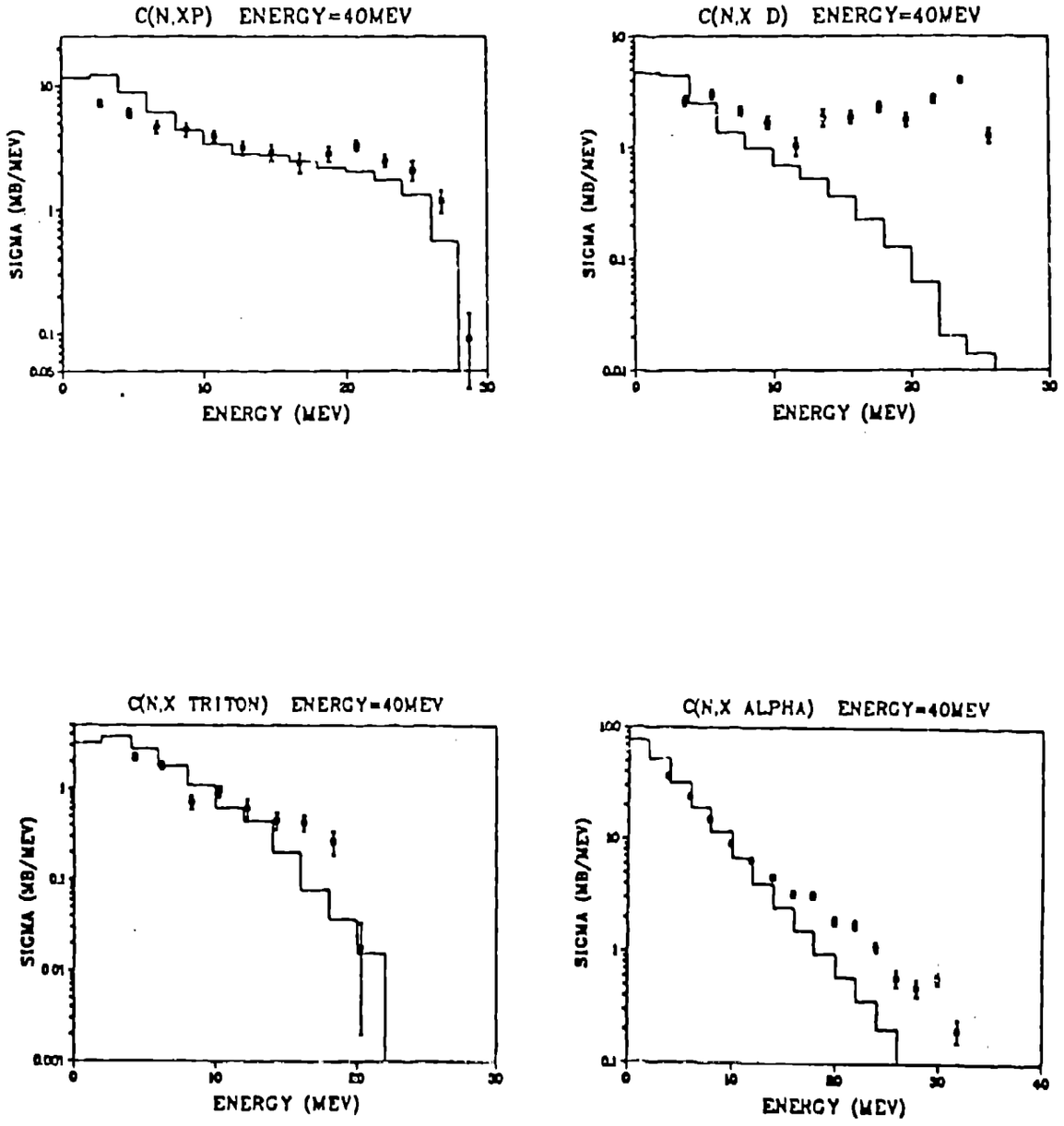

Figure 2

Comparison of calculated angle-integrated differential cross sections for 40 MeV neutrons incident on ^{12}C with the experimental results of Brady et al.[6]

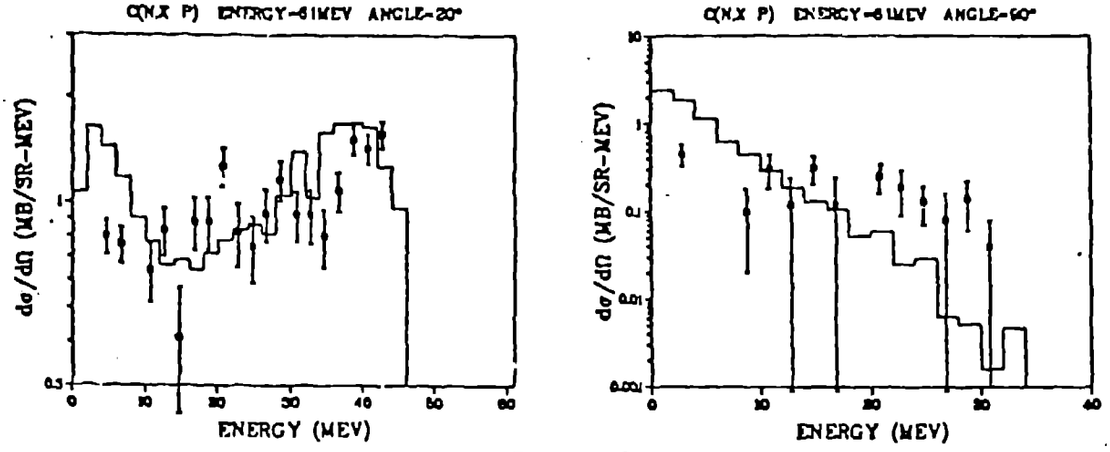

Figure 3

Comparison of calculated double differential cross sections for proton production by 61 MeV neutrons incident on ^{12}C with the experimental results of Brady et al.[6]

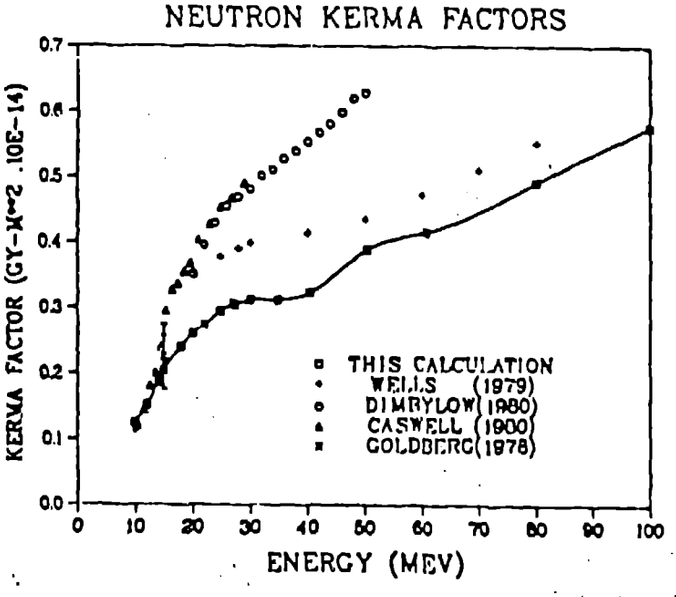

Figure 4

Calculated kerma factors for ^{12}C compared with other work.

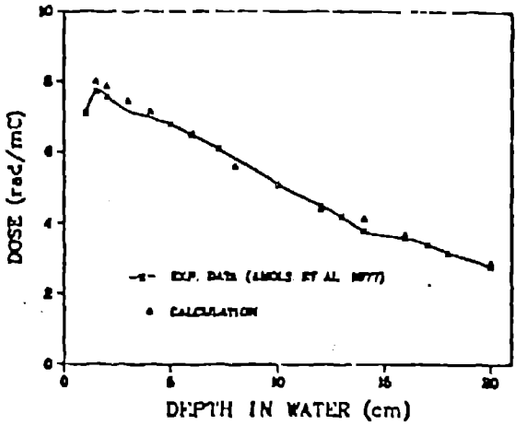

a

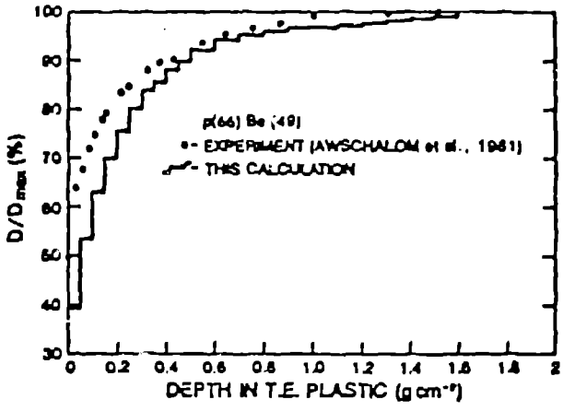

b

Figure 5

Absolute depth-dose curve for a p(65)-Be(65) beam in water for a 6.9 x 8.6 cm^2 field size.

Buildup curve for a p(66)-Be(40) beam in TE plastic for a 14.3 x 14.3 cm^2 field size.

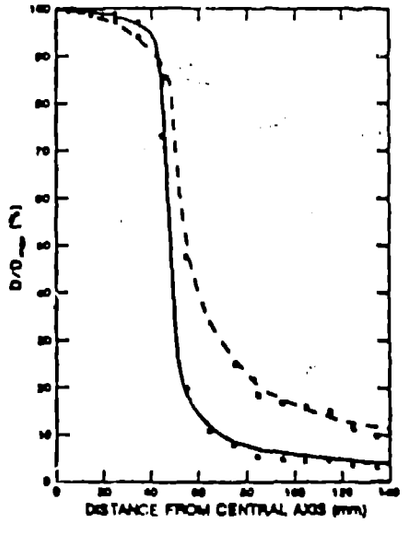

Figure 6

Off-axis dose profiles for a 5.7 x 5.7 cm^2 field size in a p(65)-Be(40) beam. The points are from this calculation; the full line (2 cm depth) and the dashed line (20 cm depth) are experimental results from Ref. 15.

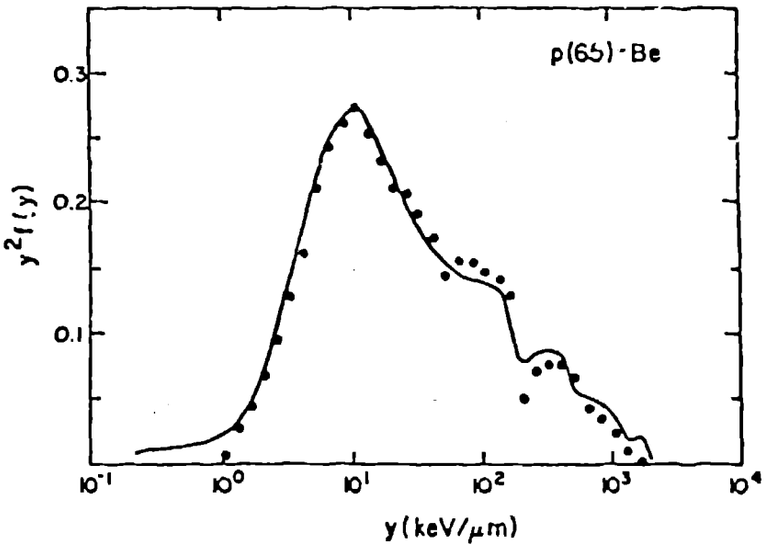

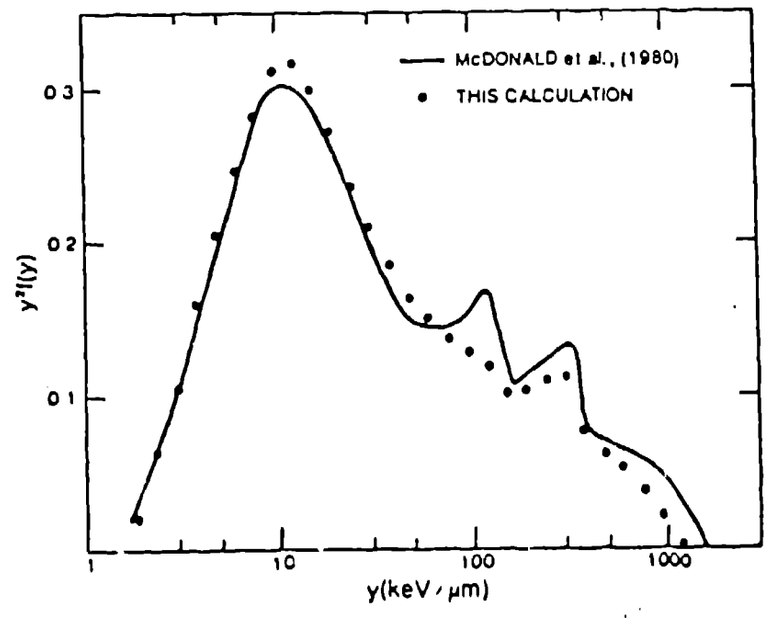

Figure 7

Microdosimetric spectra for a p(65)-Be(65) beam (upper graph) and a monoenergetic 20-MeV beam (lower graph). The full lines are experimental data from Refs. 11 and 5 and the dots are our calculation.